

# **Supplementary Information**

Michael R. Coates <sup>\*,†</sup> Ambar Banerjee <sup>,†,‡</sup> Raphael M. Jay <sup>,‡</sup> Philippe Wernet <sup>,‡</sup>  
and Michael Odelius <sup>\*,†</sup>

*†Department of Physics, Stockholm University, AlbaNova University Center, SE-106 91  
Stockholm Sweden*

*‡Department of Physics and Astronomy, Uppsala University, Box 516, SE-751 20 Uppsala,  
Sweden*

E-mail: [michael.coates@fysik.su.se](mailto:michael.coates@fysik.su.se); [odelius@fysik.su.se](mailto:odelius@fysik.su.se)

## Methods

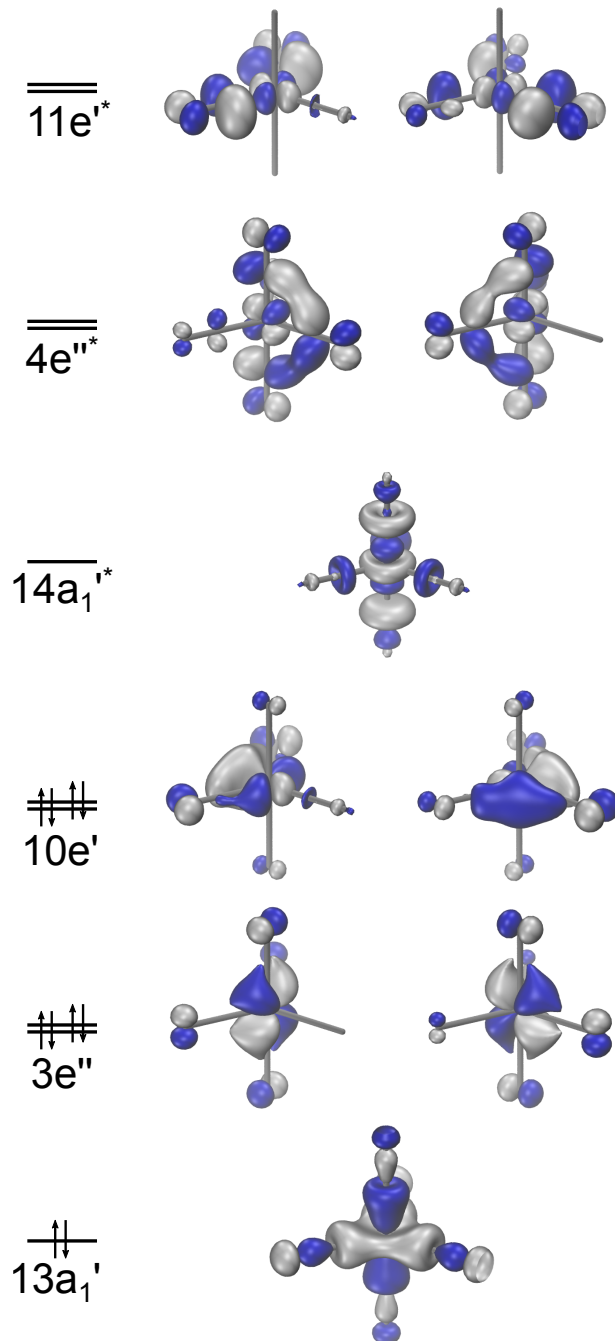


Figure S1: The CAS(10e,10o) orbitals containing the energetically relevant bonding and anti-bonding molecular orbitals of  $\text{Fe}(\text{CO})_5$ .

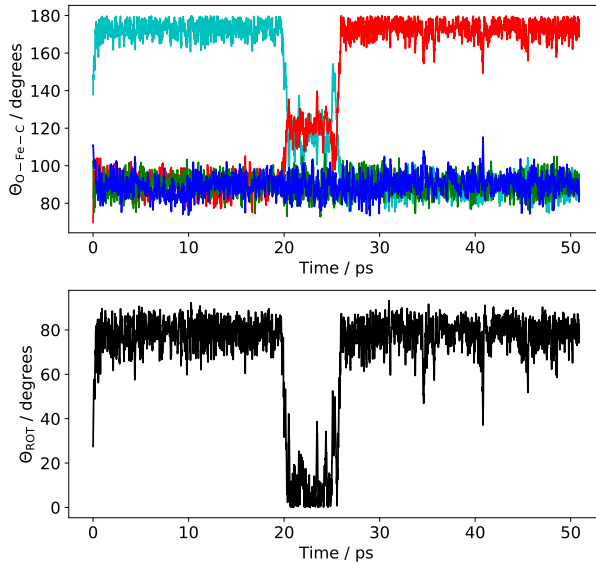


Figure S2: Top: the O-Fe-C angles ( $\Theta_{O-Fe-C}$ ) for the  $^1\text{Fe}(\text{CO})_4 - \text{OH}$  simulation including the equilibrium (0-10 ps) and production (10-50 ps) runs. The indices of the axial and equatorial ethanol oxygen and carbonyl carbon atoms were identified at 0 ps and tracked for all times. The initial simulation of  $^1\text{Fe}(\text{CO})_4 - \text{OH}$  AX is indicated by the three O-Fe-C angles of  $\sim 90^\circ$  and one O-Fe-C angle of  $\sim 180^\circ$ . The region between 20 and  $\sim 26$  ps containing two O-Fe-C angles of  $\sim 90^\circ$  and two O-Fe-C angles of  $\sim 120^\circ$  indicate the formation of  $^1\text{Fe}(\text{CO})_4 - \text{OH}$  EQ. Following this region, the ligands exchange position and re-form the  $^1\text{Fe}(\text{CO})_4 - \text{OH}$  AX complex. Bottom: The measure of the pseudo-rotation ( $\Theta_{ROT} = \max(\theta_1 - \theta_2)$ ) defined as the difference between the two largest angles which tends to zero as the  $^1\text{Fe}(\text{CO})_4 - \text{OH}$  EQ species is formed.

# Results

## Singlet and triplet reactivity

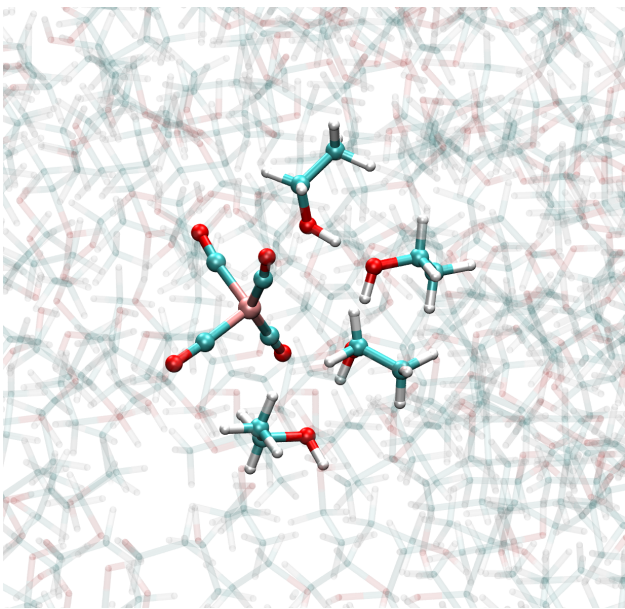


Figure S3: A qualitative picture of the solvation of  ${}^3\text{Fe}(\text{CO})_4$  indicates a small hydrogen bonding network of ethanol molecules around the weakly interacting metal complex.

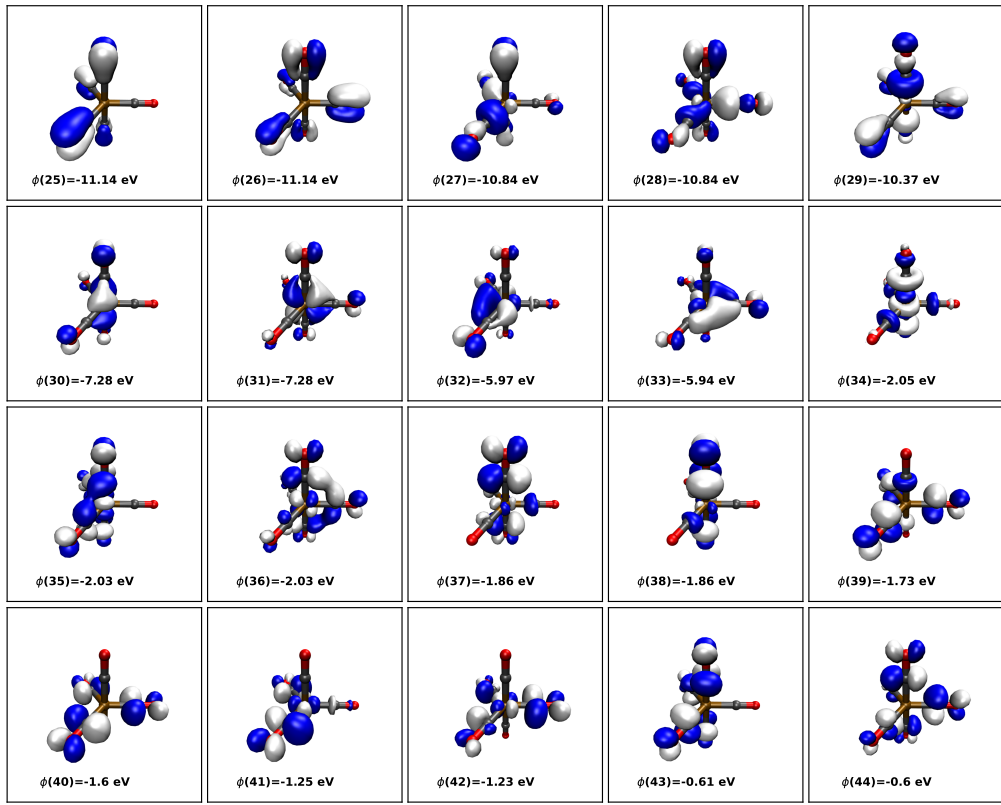


Figure S4: The energetically relevant valence molecular orbitals of  ${}^1\text{Fe}(\text{CO})_5$  plotted from the cp2k KS-DFT calculation using the BLYP functional and GTH pseudopotentials with the GTH-DZVP (Fe) and GTH-TZVP (C,O,H) basis sets. The HOMO is indicated by orbital label  $\phi(33)$ .

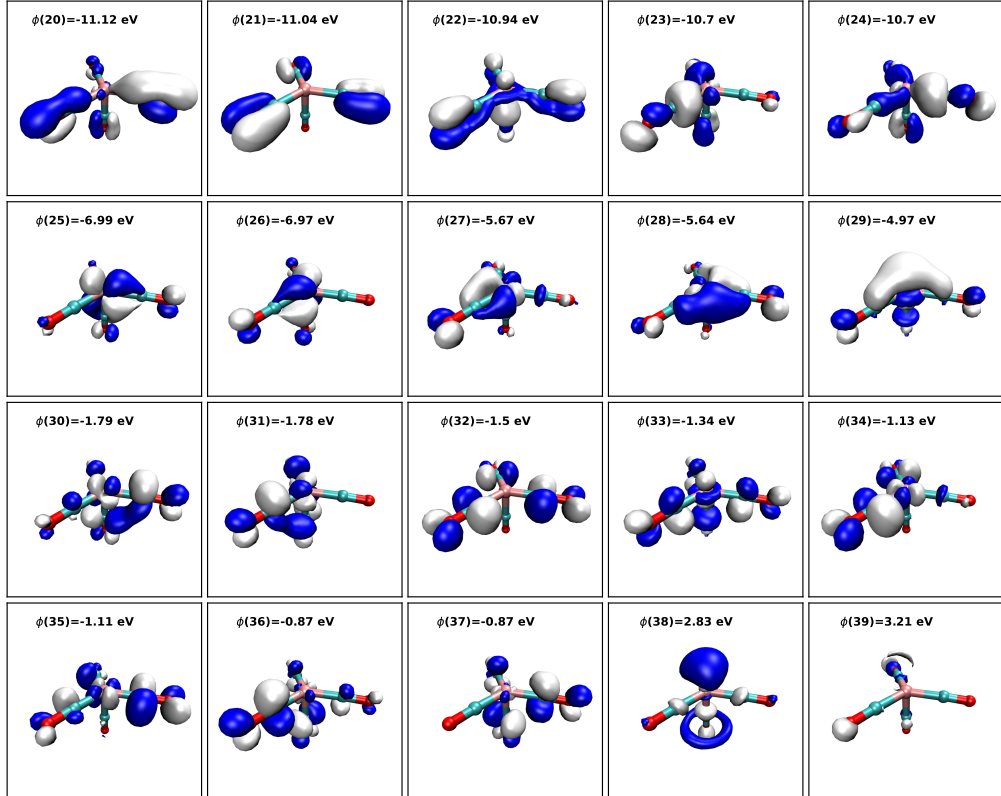


Figure S5: The energetically relevant valence molecular orbitals of  ${}^1\text{Fe}(\text{CO})_4$  AX plotted from the cp2k KS-DFT calculation using the BLYP functional and GTH pseudopotentials with the GTH-DZVP (Fe) and GTH-TZVP (C,O,H) basis sets. The HOMO is indicated by orbital label  $\phi(28)$ .

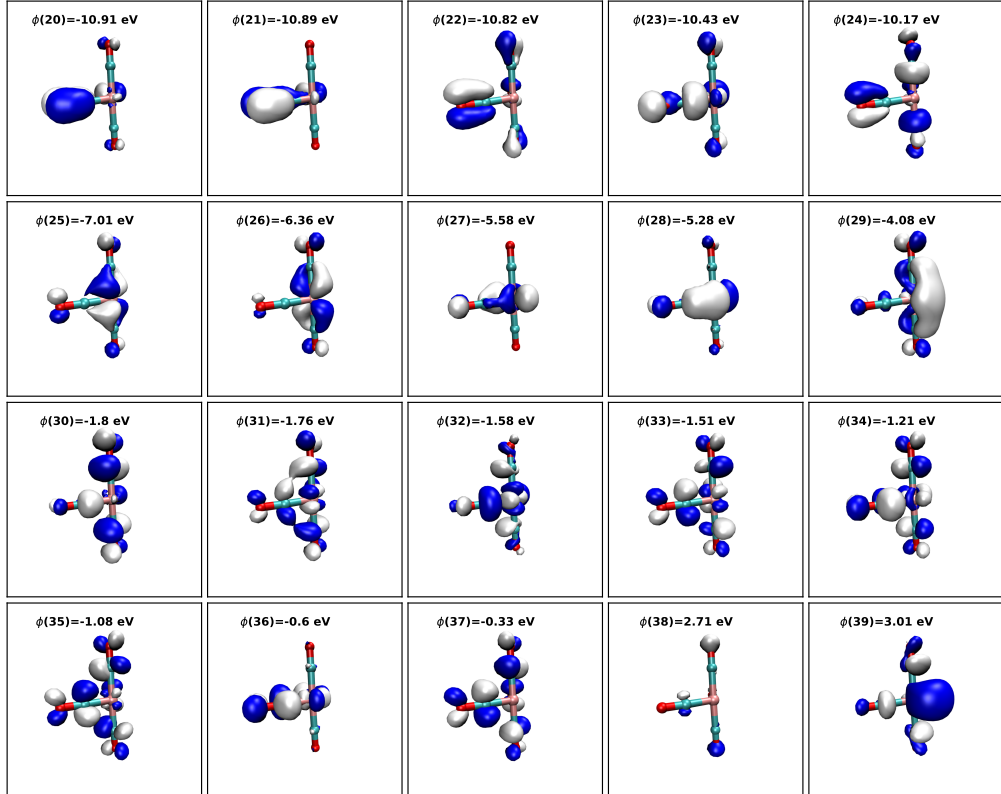


Figure S6: The energetically relevant valence molecular orbitals of  ${}^1\text{Fe}(\text{CO})_4$  EQ plotted from the cp2k KS-DFT calculation using the BLYP functional and GTH pseudopotentials with the GTH-DZVP (Fe) and GTH-TZVP (C,O,H) basis sets. The HOMO is indicated by orbital label  $\phi(28)$ .

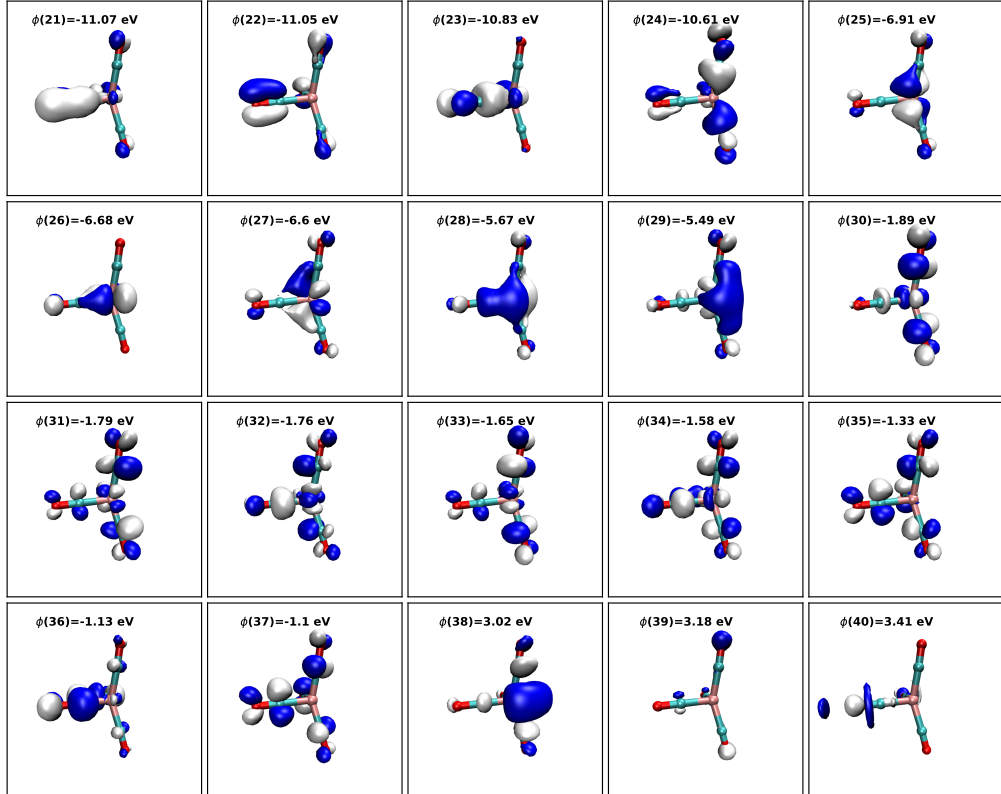


Figure S7: The energetically relevant valence molecular orbitals of  ${}^3\text{Fe}(\text{CO})_4$  ( $\alpha$ -spin) plotted from the cp2k KS-DFT calculation using the BLYP functional and GTH pseudopotentials with the GTH-DZVP (Fe) and GTH-TZVP (C,O,H) basis sets. The HOMO is indicated by orbital label  $\phi(29)$ .

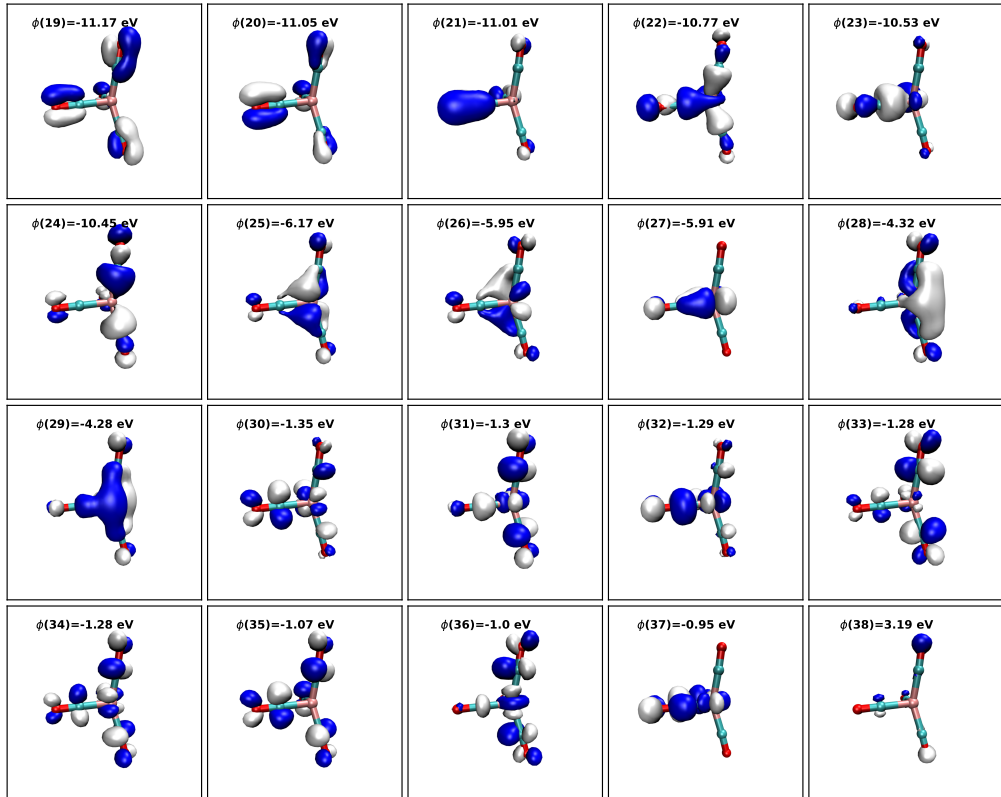


Figure S8: The energetically relevant valence molecular orbitals of  ${}^3\text{Fe}(\text{CO})_4$  ( $\beta$ -spin) plotted from the cp2k KS-DFT calculation using the BLYP functional and GTH pseudopotentials with the GTH-DZVP (Fe) and GTH-TZVP (C,O,H) basis sets. The HOMO is indicated by orbital label  $\phi(27)$ .